Available online at www.sciencedirect.com
ScienceDirect
Journal of Power Sources 159 (2006) 81–87
JOURNAL OF POWER SOURCES
www.elsevier.com/locate/jpowsour

Hydrogen storage of metal nitrides by a mechanochemical reaction

Yoshitsugu Kojima*, Yasuaki Kawai, Nobuko Ohba

Toyota Central R&D Labs. Inc., Nagakute-cho, Aichi-gun, Aichi 480-1192, Japan

Available online 23 May 2006

Abstract

Mechanochemical reaction of metal nitrides (Li_3N, Ca_3N_2, h-BN, Mg_3N_2, Si_3N_4, AlN, TiN, VN, ZrN) was performed in a planetary ball mill. We demonstrated that hydrogen (H_2) can be stored by the ball milling of their respective metal nitrides in a H_2 atmosphere at 1 MPa and room temperature. The H_2 content of ball-milled metal nitrides was 0.2–5.0 wt.%. This reaction did not occur at ambient conditions without a mechanochemical reaction mechanism. Infrared absorption showed that the N–H stretching vibrations of the ball-milled light metal nitrides occurred at 3100–3500 cm^{-1}. The N–H force constant of the metal imides in the ball-milled metal nitrides decreased with the metal ionic radius and the electronegativity. These results indicated that the size of the metal ion and the charge transfer from the metal to nitrogen play important roles for the force constant.
© 2006 Elsevier B.V. All rights reserved.

Keywords: Metal nitride; Mechanochemical reaction; Hydrogen storage; Ball mill; Infrared absorption

1. Introduction

A polymer electrolyte fuel cell (PEFC, PEM fuel cell) is the prime power source for fuel cell vehicle (FCV). One of the most widely envisioned sources of fuel for FCV is hydrogen (H_2). Therefore, it is necessary to have a storage system of H_2 and to have H_2 delivered on demand. H_2 can be stored in tanks as compressed or liquefied H_2 or by adsorption on carbon materials [1,2]. It can also be stored in H_2-absorbing alloys, H_2-absorbing alloys with high dissociation pressure [3,4] or as a chemical hydride, such as $NaBH_4$ [5–7], $LiBH_4$ [8,9], $NaAlH_4$ [10,11] or MgH_2 [12–14], as well as in an organic hydride, such as methylcyclohexane or decalin [15]. In recent years, attention has been given to metal nitrides [16–21]. Chen et al. reported that metal nitride (Li_3N) absorbed and desorbed hydrogen at high temperature (468–528 K) [16]. It has been reported that the partial substitution of lithium by magnesium in the nitride/imide system (Li–Mg–N–H) destabilizes Li–N–H system [17–21]. For useable H_2 storage, H_2 absorption/desorption at ambient temperature is necessary. Recently, it has been shown that chemical reaction can occur at room temperature during mechanochemical processing [22].

In this paper, we demonstrate that hydrogen can be stored by the process of ball milling metal nitrides in a H_2 atmosphere at a pressure of 1 MPa and at room temperature.

2. Experimental

2.1. Materials

Lithium nitride Li_3N (Kojundo Chemical Laboratory Co. Ltd., Japan, molecular weight: 34.82, density: 1.38 g cm^{-3}, purity: >99%), calcium nitride Ca_3N_2 (Sigma–Aldrich, molecular weight: 148.25, density: 2.63 g cm^{-3}, purity: >99%) hexagonal boron nitride h-BN (Kojundo Chemical Laboratories Co. Ltd., molecular weight: 24.82, density: 2.25 g cm^{-3}, purity: >99%), magnesium nitride Mg_3N_2 (Sigma–Aldrich, molecular weight: 100.95, density: 2.71 g cm^{-3}, purity: >99.5%), aluminum nitride AlN (Kojundo Chemical Laboratories Co. Ltd., molecular weight: 41.0, density: 3.26 g cm^{-3}, purity: 99.9%), silicon nitride Si_3N_4 (Kojundo Chemical Laboratories Co. Ltd., molecular weight: 140.28, density: 3.44 g cm^{-3}purity: >99.9%), titanium nitride TiN (Kojundo Chemical Laboratories Co. Ltd., molecular weight: 61.91, density: 5.43 g cm^{-3}, purity: 99%), vanadium nitride VN (Sigma–Aldrich, molecular weight: 64.95, density: 6.13 g cm^{-3}, purity: 99%), and zirconium nitride ZrN (Sigma–Aldrich, molecular weight: 105.23, density: 7.09 g cm^{-3}) were used in this experiment. Lithium amide $LiNH_2$ (Sigma–Aldrich, molecular weight: 22.96,

* Corresponding author. Tel.: +81 561 63 5325; fax: +81 561 63 6137.
E-mail address: kojima@mosk.tytlabs.co.jp (Y. Kojima).

0378-7753/$ – see front matter © 2006 Elsevier B.V. All rights reserved.
doi:10.1016/j.jpowsour.2006.04.024

density 1.17 g cm^{-3}) and borane–ammonia complex NH_3BH_3 (Sigma–Aldrich, molecular weight 30.87, purity 90%) were used as reference specimens. High purity H_2 gas (>99.99999%) was used as the reaction atmosphere. Mechanochemical reaction was performed in a planetary ball mill (Fritsch P-5). The mill container (Cr–Mo steel pot with an internal volume of 300 mL) was loaded with 5 g of metal nitride and 40 pieces of steel ball with a diameter of 9.5 mm (ball-to-powder mass ratio of 28:1). The metal nitrides were milled at 400 rpm of rotational speed and 200 rpm of revolutional speed for 20 h in a H_2 gas atmosphere at a pressure of 1 MPa and room temperature (296 K).

2.2. Characterization

ThermoNicolet AVATAR 360 E.S.P. FT-IR spectrometer with ATR system was used for IR studies in an inert atmosphere of N_2. X-ray diffraction intensity curves in an inert atmosphere (Ar) were recorded with Cu Kα radiation (50 kV, 300 mA) filtered by monochrometer using Rigaku Rint-TTR. The apertures of the first, second and third slits were 0.5, 0.5 and 0.15 mm, respectively. With the Horiba EMGA-621 Hydrogen Analyzer, H_2 contained in a specimen was extracted by heating at 2273 K in an inert gas (Ar). The decomposed H_2 was released from the specimen and was monitored by a thermal conductivity detector.

Hydrogen absorption properties of the metal nitrides were measured with a commercial pressure–composition–temperature (PCT) automatic measuring system provided by Suzuki Shokan Co. Ltd., Japan (Sievert's type apparatus).

3. Results and discussion

The products after ball milling of Li_3N and Ca_3N_2 were light brown, which are different from the dark brown starting materials [23]. Fig. 1 shows the H_2 contents for various ball-milled metal nitrides. We found that H_2 can be stored by the ball milling of their respective metal nitrides in a H_2 atmosphere at 1 MPa and room temperature. The values differ significantly between the different specimens. It is shown that the ball-milled light metal nitrides such as Li_3N and Ca_3N_2 have the H_2 contents above 3 wt.% while the small amounts of H_2 are stored after the transition metal nitrides have been milled under H_2 pressure (0.2–0.5 wt.%). The H_2 absorption properties at 9 MPa and room temperature for 20 h were evaluated by the Sievert's apparatus. The H_2 content was also monitored by a hydrogen analyzer. The measurements confirmed that the metal nitrides did not absorb H_2 without a mechanical milling.

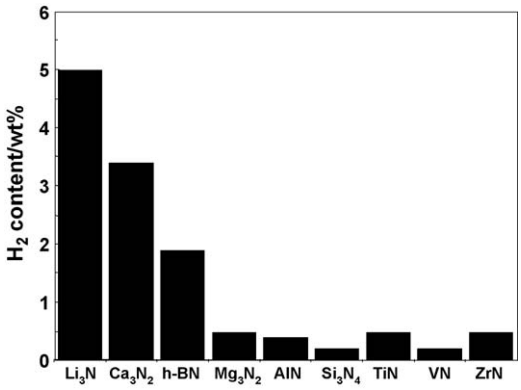

Fig. 1. H_2 content of different ball-milled metal nitrides.

The H_2 absorption during milling suggests that the hydrogenation process is a two-step process as follows. H_2 is absorbed on new particle surfaces created by pulverization during initial milling. The absorbed H_2 reacts with metal nitrides such as Li_3N and Ca_3N_2 to form metal imides, metal amides and metal hydrides under further high-energy ball impacts as shown following sections. Local temperature rise, induced by ball impacts, may also contribute to the hydrogenation reaction.

3.1. Ball-milled Li_3N [23]

The total H_2 content in ball-milled Li_3N determined by a hydrogen analyzer was 5.0 wt.% after milling for 20 h. Fig. 2 presents the XRD profiles of the ball-milled Li_3N, Li_3N together with the data of Li_2NH, $LiNH_2$, LiH, Li_2O and LiOH. The diffraction peaks of the ball-milled Li_3N at 2θ of 38.3°, 44.5° and 64.8° are raised from (1 1 1), (2 0 0) and (2 2 0) planes of LiH in which its unit cell is cubic in shape [24]. The XRD profiles also show that the ball-milled Li_3N includes unreacted Li_3N. The unit cell of Li_2NH is cubic in shape [24] and the unit cell of $LiNH_2$ is tetragonal in shape [24]. As the XRD curve of $LiNH_2$ phase is quite similar to that of Li_2NH phase, it is difficult to characterize the hydrogenating reaction during ball milling only from the XRD curves. The strongest peak of the ball-milled Li_3N in the XRD curve is at about 33° and which comes from either Li_2O or LiOH. The O–H stretching vibration associated with LiOH however, was not observed in the IR spectrum. This contamination might originate from small leaks in the pulverizing system.

The structure of ball-milled Li_3N was investigated by infrared spectroscopy. Fig. 3 shows the infrared absorption spectra of ball-milled Li_3N, Li_3N, $LiNH_2$ and Li_2NH. Here, Li_2NH was synthesized by decomposing $LiNH_2$ at 673 K under vacuum

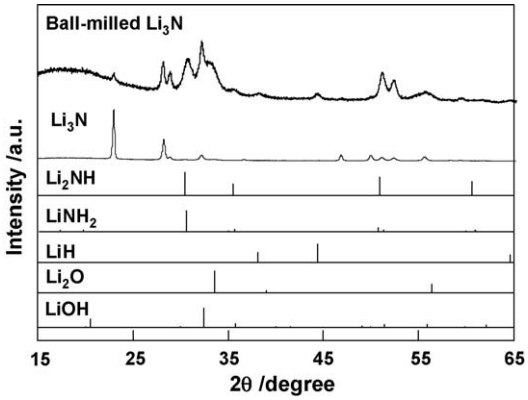

Fig. 2. XRD patterns of ball-milled Li_3N in H_2 and Li_3N together with the data of LiH (JCPDS file No. 09-0189), Li_2NH (JCPDS file No. 06-0417), $LiNH_2$ (JCPDS file No. 06-0418), Li_2O (JCPDS file No. 12-0254) and LiOH (JCPDS file No. 32-0564). The background broad diffraction in the XRD profiles is due to a polymer film used for shielding from air and H_2O.

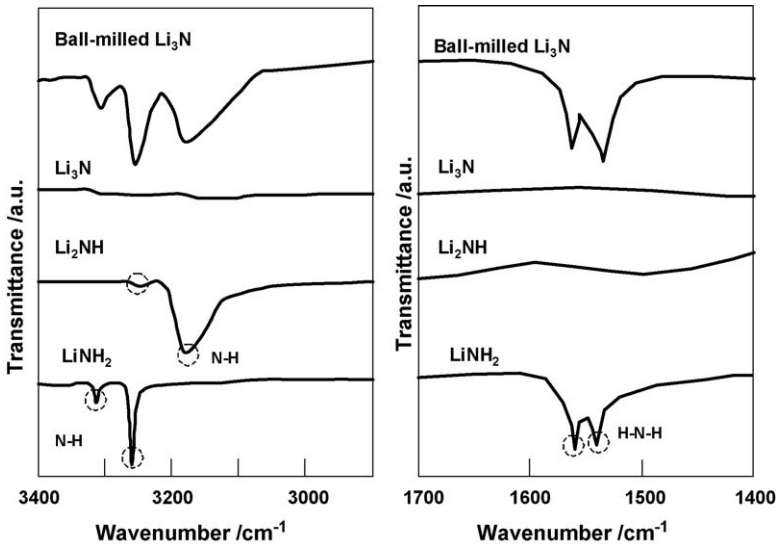

Fig. 3. Infrared absorption spectra of ball-milled Li_3N in H_2 and Li_3N together with the data of Li_2NH and $LiNH_2$.

(0.1 Pa) for 1 h [25]. The N–H symmetric and asymmetric stretching vibrations of $LiNH_2$ occur at 3260 and 3315 cm^{-1}, respectively [26]. The bands at 1540 and 1560 cm^{-1} indicate the N–H deformation vibrations of the amide ion [26]. Li_2NH gives rise to characteristic N–H stretching vibration at 3180 cm^{-1} [27,28] and small absorption at 3250 cm^{-1}. We notice that the ball-milled Li_3N contains Li_2NH and $LiNH_2$ due to the presence of these characteristic IR bands at 3180, 3260, 3320, 1540 and 1560 cm^{-1}. Those bands are broad and they can be explained by the small size of the crystallites and/or disorder of the crystallites. Thus, the Infrared absorption spectra and the X-ray diffraction (XRD) intensity curves showed that the ball-milled Li_3N is a mixture which includes Li_3N, Li_2NH and $LiNH_2$ and LiH. Then the hydrogen storage in Li_3N takes the following two-step reaction path [16]:

$$Li_3N + 2H_2 \leftrightarrow Li_2NH + LiH + H_2 \quad (1)$$

$$Li_2NH + LiH + H_2 \leftrightarrow LiNH_2 + 2LiH \quad (2)$$

H_2 of 10.4 wt.% [$2H_2/Li_3N + 2H_2$] can be stored in this reaction. The H_2 content of the ball-milled Li_3N determined using the hydrogen analyzer was 5.0 wt.% and half of the theoretical value. The calculated standard enthalpy change (heat of formation) for Eq. (1) was -116 kJ mol^{-1} H_2 [16]. Thermodynamic analysis was performed over the Li_2NH system [Eq. (2)]. Using the van't Hoff plots, the heat of formation of the H_2 absorption and desorption was about -66 kJ mol^{-1} H_2 [16,28]. These negative values indicate that Li_3N and ($Li_2NH + LiH$) can easily absorb hydrogen at room temperature. We speculate that insufficient H_2 was supplied in Li_3N powder, thus unreacted Li_3N remained due to the decrease in the H_2 content during the ball milling.

3.2. Ball-milled Ca_3N_2 [23]

The H_2 content of ball-milled Ca_3N_2 examined using a hydrogen analyzer was 3.2 wt.%. The structure of the ball-milled Ca_3N_2 was characterized by X-ray diffraction method and infrared spectroscopy. The XRD patterns of ball-milled Ca_3N_2 and as received Ca_3N_2, together with the data of Ca_2NH, CaNH, CaH_2, $Ca(NH_2)_2$ are shown in Fig. 4. Fig. 4 indicates that the ball-milled Ca_3N_2 in H_2 does not contain unreacted Ca_3N_2. We notice that the diffraction peaks of the ball-milled Ca_3N_2 at 2θ of 27.9°, 30.1°, 31.8°, 41.5° and 60.0° are raised from (0 1 1), (2 0 0), (1 1 1), (2 1 1), (2 0 2) planes of CaH_2, in which the unit cell of CaH_2 is orthorhombic in shape [24]. The ball-milled Ca_3N_2 also includes Ca_2NH or CaNH because the unit cells of Ca_2NH and CaNH are cubic in shape [24] and their XRD curves are similar to each other.

The crystal structures of CaNH and Ca_2NH are given in Fig. 5 with respect to generating of a possible N–H bond. The crystal structure of CaNH generated from XRD indicates the presence of N–H bond, but the crystal structure of Ca_2NH generated by XRD shows that Ca_2NH does not have that bond. Fig. 6 shows the infrared absorption spectra of ball-milled Ca_3N_2 and Ca_3N_2. The ball-milled Ca_3N_2 now contains a stretch at 3130 cm^{-1} which is due to the presence of CaNH. Thus the reaction of Ca_3N_2 and

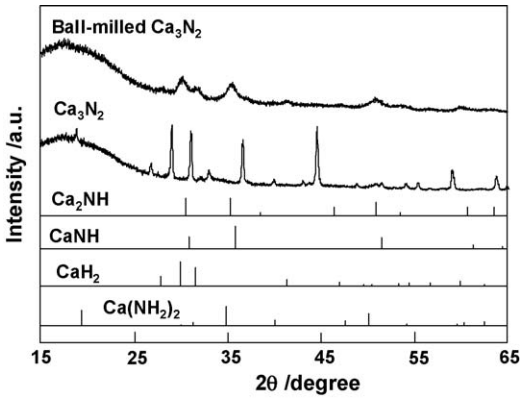

Fig. 4. XRD patterns of ball-milled Ca_3N_2 in H_2 and Ca_3N_2 together with the data of CaH_2 (JCPDS file No. 03-065-2384), Ca_2NH (JCPDS file No. 26-0308), CaNH (JCPDS file No. 01-075-0430) and $Ca(NH_2)_2$ (JCPDS file No. 16-0476).

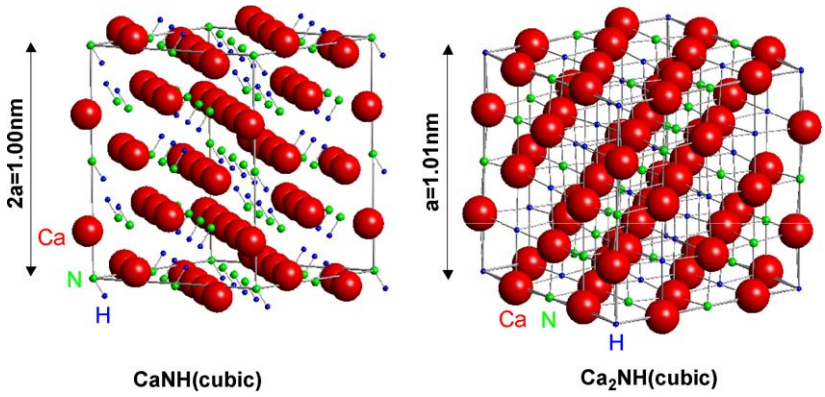

Fig. 5. Crystal structures of CaNH and Ca_2NH.

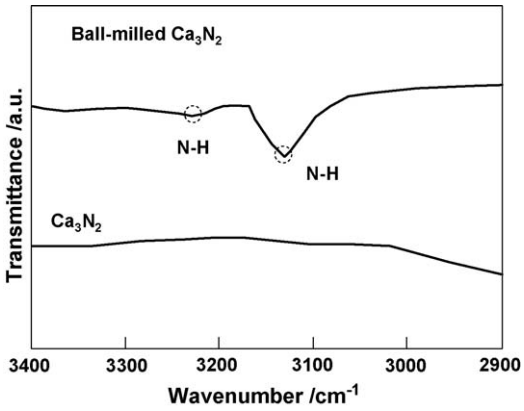

Fig. 6. Infrared absorption spectra of ball-milled Ca_3N_2 in H_2 and Ca_3N_2.

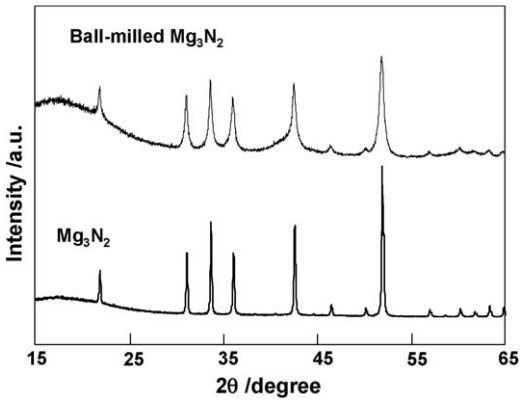

Fig. 7. XRD patterns of ball-milled Mg_3N_2 and Mg_3N_2.

H_2 by the mechanochemical reaction can be expressed by Eqs. (3) and (4):

$$Ca_3N_2 + 4H_2 \leftrightarrow 2CaNH + CaH_2 + 2H_2 \quad (3)$$

$$2CaNH + CaH_2 + 2H_2 \leftrightarrow Ca(NH_2)_2 + 2CaH_2 \quad (4)$$

The theoretical H_2 content obtained by Eqs. (3) and (4) is 5.2 wt.% [$4H_2/(Ca_3N_2 + 4H_2)$]. The H_2 content of ball-milled Ca_3N_2 examined using a hydrogen analyzer was 3.2 wt.% and this value is a little large compared with the theoretical value of 2.7 wt.% by Eq. (3) [$2H_2/(Ca_3N_2 + 4H_2)$]. The difference is due to the fact that the ball-milled Ca_3N_2 includes a small amount of $Ca(NH_2)_2$.

According to the first-principle calculations [29], it is reported that the calculated values of the heat of formation of Eqs. (3) and (4) are −115 and −57 kJ mol^{-1} H_2, respectively. The large negative heat of formation indicates that CaH_2, CaNH and $Ca(NH_2)_2$ are stable with respect to Ca_3N_2, while the reaction [Eq. (4)] does not proceed easily. We assumed that the activation energy for the reaction is larger than the Li–N–H system [Eq. (2)].

3.3. Ball-milled Mg_3N_2

Fig. 7 shows the XRD patterns of ball-milled Mg_3N_2 and Mg_3N_2. The unit cell of Mg_3N_2 is cubic in shape [24] and the crystal structure of Mg_3N_2 maintained after ball milling. The ball-milled Mg_3N_2 displays a broader diffraction peak. Judging from Fig. 7, the ball-milled Mg_3N_2 serves the formation of the small size of the crystallites and/or disorder of the crystallites compared with Mg_3N_2.

It has been reported that MgNH gives rise to a characteristic band around 3226 cm^{-1} [30]. The N–H stretching mode of MgNH shifts to lower energy compared to $Mg(NH_2)_2$ (3277, 3329 cm^{-1}) [30]. The broad IR band of the ball-milled Mg_3N_2 is observed at 3160 cm^{-1} as shown in Fig. 8 and is approximately in agreement with that of MgNH. Using an analogy similar to

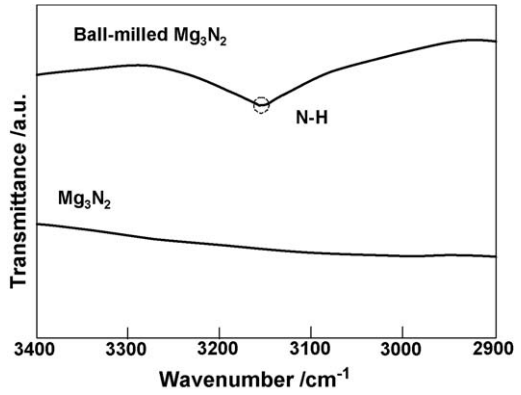

Fig. 8. Infrared absorption spectra of ball-milled Mg_3N_2 and Mg_3N_2.

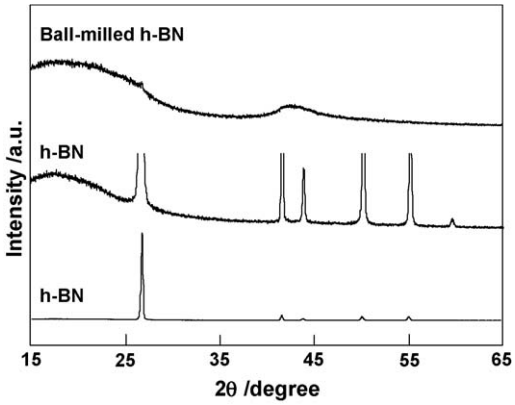

Fig. 9. XRD patterns of ball-milled h-BN and h-BN.

Eqs. (3) and (4), the hydriding reaction of Mg_3N_2 is as follows [31]:

$$Mg_3N_2 + 4H_2 \leftrightarrow 2MgNH + MgH_2 + 2H_2 \quad (5)$$

$$2MgNH + MgH_2 + 2H_2 \leftrightarrow Mg(NH_2)_2 + 2MgH_2 \quad (6)$$

The experimental H_2 content of the ball-milled Mg_3N_2 is 0.5 wt.%. The theoretical value is 7.4 wt.% [$4H_2/(Mg_3N_2 + 4H_2)$]. Thus only 7% H_2 content was obtained. Values for the heat of formation in Eqs. (5) and (6) by the first principles calculation were -2 and -43 kJ mol^{-1} H_2, respectively [29]. The small absolute values correspond to high dissociation pressure. The high dissociation pressure and the high activation energy may prevent the hydriding reaction.

3.4. Ball-milled h-BN

The XRD patterns of ball-milled h-BN and h-BN are shown in Fig. 9. As h-BN is mechanically milled, it shows diffuse diffraction peaks at 2θ of 26.7° and 42.6°, corresponding to the (0 0 2) and (1 0 0) planes for h-BN. The (0 0 2) peak of h-BN based on the interlayer spacing weakens by milling. This indicates that the form of the interlayer structure of h-BN is drastically changed by mechanical milling. The H_2 content in ball-milled h-BN is 1.9 wt.%, being comparable to the value reported by Wang et al. [32] and is only 10% of the corresponding theoretical value of NH_3BH_3 (19.6 wt.%). The infrared spectrum of the ball-milled h-BN is shown in Fig. 10. Characteristic N–H and B–H stretching vibrations of the spectrum appear at 3440 and 2520 cm^{-1}. The N–H and B–H stretching modes shift to higher energy compared with borane–ammonia complex (NH_3BH_3, N–H: 3302 cm^{-1}, B–H: 2313 cm^{-1}). Another distinct difference of ball-milled BN and NH_3BH_3 was observed in the B–N stretch with a strong peak at 1326 cm^{-1} for the ball-milled h-BN and a slight peak at 1374 cm^{-1} for NH_3BH_3 [33]. The B–N absorption of ball-milled B–N resembles that of BN (1279 cm^{-1}). In addition, out of plane B–N–B absorption at 784, 757 cm^{-1} of ball-milled h-BN and h-BN indicates the presence of B_3N_3 ring structure [33]. To interpret the hydride reaction, it is convenient to describe the N–H and B–H stretching vibrations in terms of addition reaction of H_2 at the edge of the h-BN produced by mechanical milling in a H_2 atmosphere as indicated in Fig. 10.

Ball-milled AlN, Si_3N_4 and transition metal nitrides also showed broad diffraction peaks. These broad peaks also establish the small size of the crystallites and/or disorder of the crystallites.

3.5. Infrared absorption spectra of light metal nitrides

The IR bands of ball-milled AlN, and Si_3N_4 also appeared at 3210 and 3330 cm^{-1}, respectively (Fig. 11). The bands are assigned to the N–H stretching vibrations [34]. Thus we found that the infrared spectra of the ball-milled light metal nitrides show N–H stretching vibrations around 3100–3500 cm^{-1}.

The simple N–H stretching vibrations of the metal imides in ball-milled metal nitrides can be approximated by considering the atoms as point masses linked by a spring having a force constant k and Hooke's Law. Using this simple approximation, the stretching frequency of the molecule vibration (wave number) of two atoms system would give the result:

$$\nu = k^{1/2}/(2\pi c)[1/m_N + 1/m_H]^{1/2} \quad (7)$$

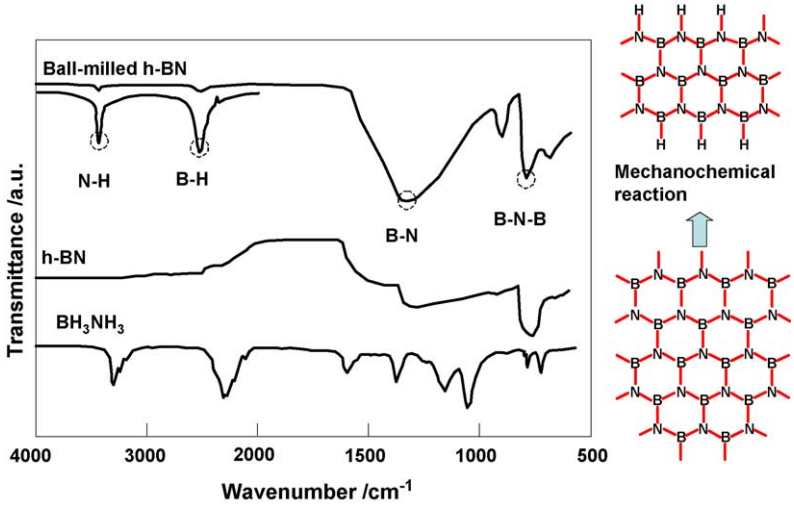

Fig. 10. Infrared absorption spectra of ball-milled BN, BN and NH_3BH_3.

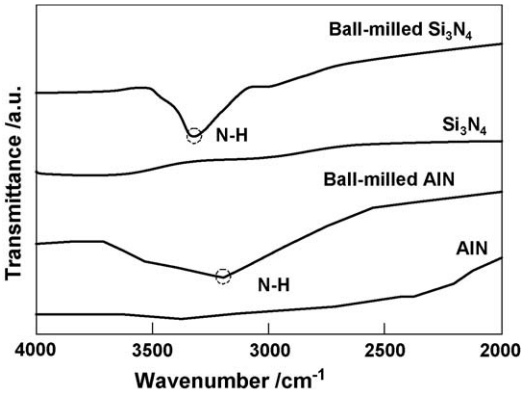

Fig. 11. Infrared absorption spectra of ball-milled AlN, AlN, ball-milled Si_3N_4 and Si_3N_4.

where ν is wave number(cm^{-1}), c speed of light ($cm\,s^{-1}$), k force constant (dyne cm^{-1}), m_N mass for nitrogen atom ($g\,atom^{-1}$) and m_H is mass for hydrogen atom ($g\,atom^{-1}$). Note that this formula holds for a harmonic oscillator.The force constant k is expressed as

$$k = \nu^2(4\pi^2c^2)[m_N m_H/(m_H + m_N)] \times 10^{-3}\,[N\,m^{-1}] \quad (8)$$

where c, m_N and m_H are $3 \times 10^{10}\,cm\,s^{-1}$, 23.3×10^{-24} and $1.66 \times 10^{-24}\,g\,atom^{-1}$, respectively. Substituting experimental values of the wave number in Eq. (8), the force constants were given. Here, we assumed that metal imides are synthesized by the mechanochemical reaction of AlN and Si_3N_4.

Linde et al. reported that force constants of metal imides exhibit a linear decrease with the ionic radius [30]. Fig. 12 shows the plot of the force constant for the ball-milled metal nitrides against the ionic radius of the metal combined with nitrogen [30,35]. The force constant decreases with the radius. The force constant also depends on the electronegativity of the metal [36]. So, It was confirmed that the force constant decreased with the ionic radius at the same electronegativity (Li: 1.0, Ca: 1.0) [36]. It was reported that the N–H stretching modes in IR spectra of $LiNH_2$ were shifted to higher energy as a result of the coordination by Li^+ ion and the repulsion of neighboring anions [26]. A larger sized cation gives a smaller N–H bond force constant because of the longer bond length between N and H by the weakened repulsion from protons of neighboring imide ions. Li and Mg have similar ionic radius (Li: 0.068 nm, Mg: 0.065 nm), but the higher electronegativity of Mg than that of Li provides smaller force constant. This result indicates that the control of the charge transfer from a cation to N–H leads to a small N–H bond force constant.

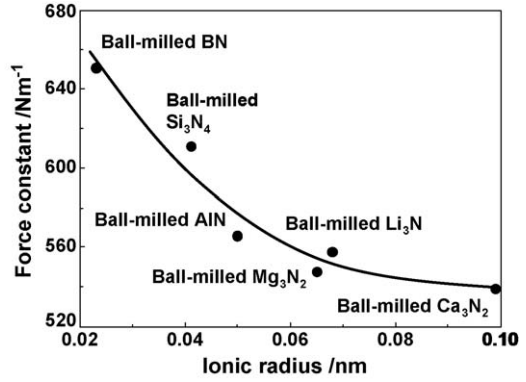

Fig. 12. Ionic radius dependence of force constant for ball-milled metal nitrides.

A dramatic reduction in hydrogen desorption temperatures were observed in the Li–Mg–N–H and Li–Ca–N–H systems compared with Li–N–H system [17–20]. Generally, a bond energy U is proportional to a force constant k [37]:

$$U \propto k \quad (9)$$

Thus, partial cation substitutions such as Mg^{2+} and Ca^{2+} using larger electronegativity and ionic radius may provide lower hydrogen desorption temperature in Li–Mg–N–H and Li–Ca–N–H systems based on their weak N–H bond energy.

4. Conclusions

Hydrogen can be stored by a mechanochemical reaction of their respective metal nitrides in a H_2 atmosphere at room temperature. The H_2 content of ball-milled metal nitrides were 0.2–5 wt.%. Infrared absorption showed that the N–H stretching vibration of the ball-milled light metal nitrides occurred around 3100–3500 cm^{-1}. It was indicated that the size of the metal ion and the charge transfer from the metal to nitrogen play important roles for the force constant.

Acknowledgements

The authors are greatly indebted to Dr. G.J. Shafer, Y. Kondo, M. Aoki, T. Noritake, Dr. K. Miwa and Dr. S. Towata of the Toyota Central R&D Labs. Inc., for their help and discussion.

References

[1] R. Chahine, T.K. Bose, Int. J. Hydrogen Energy 19 (1994) 161–164.
[2] Y. Kojima, N. Suzuki, Appl. Phys. Lett. 84 (2004) 4113–4115.
[3] Y. Kojima, Y. Kawai, S. Towata, T. Matsunaga, T. Shinozawa, M. Kimbara, Materials and Technology for Hydrogen Storage and Generation, Materials Research Society Symposium Proceedings, 28–31 March, 2005 (in preparation).;
Y. Kojima, Y. Kawai, S. Towata, T. Matsunaga, T. Shinozawa, M. Kimbara, Collected Abstracts of the 2004 Autumn Meeting of the Japan Institute of Metals, p. 157.
[4] D. Mori, N. Kobayashi, T. Matsunaga, K. Toh, Y. Kojima, Mater. Jpn. 44 (2005) 257.
[5] S.C. Amendola, S.L. Sharp-Goldman, M.S. Janjua, M.T. Kelly, P.J. Petillo, M. Binder, J. Power Sources 85 (2000) 186–189.
[6] Y. Kojima, K. Suzuki, K. Fukumoto, M. Sasaki, T. Yamamoto, Y. Kawai, H. Hayashi, Int. J. Hydrogen Energy 27 (2002) 1029–1034.
[7] Z.P. Li, B.H. Liu, K. Arai, N. Morigazaki, S. Suda, J. Alloys Compd. 356–357 (2003) 469–474.
[8] A. Züttel, P. Wenger, S. Rentsch, P. Sudan, P. Mauron, C. Emmenegger, J. Power Sources 118 (2003) 1–2.
[9] Y. Kojima, Y. Kawai, M. Kimbara, H. Nakanishi, S. Matsumoto, Int. J. Hydrogen Energy 29 (2004) 1213–1217.
[10] B. Bogdanović, M. Schwickardi, J. Alloys Compd. 253–254 (1997) 1–9.
[11] M. Fichtner, J. Engel, O. Fuhr, O. Kircher, O. Rubner, Mater. Sci. Eng. B 108 (2004) 42–47.
[12] Y. Kojima, K. Suzuki, Y. Kawai, J. Mater. Sci. Lett. 39 (2004) 2227–2229.

[13] Y. Kojima, Y. Kawai, T. Haga, in: T. Vogt, R. Stumpf, M. Heben, I. Robertson (Eds.), Symposium N Materials for Hydrogen Storage, Materials Research Society Symposium Proceedings, 2004, p. 837.
[14] N. Hanada, T. Ichikawa, H. Fujii, J. Phys. Chem. B 109 (2005) 7188–7194.
[15] E. Newson, T. Haueter, P. Hottinger, F. Von Roth, G.W.H. Scherer, T.H. Schucan, Int. J. Hydrogen Energy 23 (1998) 905–909.
[16] P. Chen, Z. Xiong, J. Luo, J. Lin, K.L. Tan, Nature 420 (2002) 302–304.
[17] Y. Nakamori, S. Orimo, J. Alloys Compd. 370 (2004) 271–275.
[18] H.Y. Leng, T. Ichikawa, S. Hino, N. Hanada, S. Isobe, H. Fujii, J. Phys. Chem. B 108 (2004) 8763–8765.
[19] W. Luo, J. Alloys Compd. 381 (2004) 284–287.
[20] S. Orimo, Y. Nakamori, G. Kitahara, K. Miwa, N. Ohba, T. Noritake, S. Towata, Appl. Phys. A 79 (2004) 1765–1767.
[21] Z. Xiong, G. Wu, J. Hu, P. Chen, Adv. Mater. 16 (2004) 1522–1525.
[22] V.P. Balema, J.W. Wiench, M. Pruski, V.K. Pecharsky, J. Am. Chem. Soc. 124 (2002) 6244–6245.
[23] Y. Kojima, Y. Kawai, Chem. Commun. (2004) 2210–2211.
[24] T.M. Kahmer (Publication Manager), W.F. McClune (Editor-in-Chief), S.N. Kabekkodu (Editor of Calculated Patterns), H.E. Clark (Staff Scientist), Powder Diffraction File, International Centre for Diffraction Data (JCPDS), Pennsylvania, USA, 2004.
[25] T. Ichikawa, S. Isobe, N. Hanada, H. Fujii, J. Alloys Compd. 365 (2004) 271–276.
[26] J.-P.O. Bohger, R.R. Eβman, H. Jacobs, J. Molecular Struct. 348 (1995) 325–328.
[27] P. Chen, Z. Xiong, J. Luo, J. Lin, K.L. Tan, J. Phys. Chem. B 107 (2003) 10967–10970.
[28] Y. Kojima, Y. Kawai, J. Alloys Compd. 395 (2005) 236–239.
[29] Report of the New Energy and Industrial Technology Development Organization (NEDO), Basic Technology Development Project for Hydrogen Safety and Utilization, Developments of lithium-based hydrogen storage materials for fuel cell vehicles, 04000549-0, 2003–2004.
[30] V.G. Linde, R. Juza, Anorg. Allg. Chem. 409 (1974) 199–214.
[31] Y. Nakamori, G. Kitahara, S. Orimo, J. Power Sources 138 (2004) 309–312.
[32] P. Wang, S. Orimo, T. Matsushima, H. Fujii, Appl. Phys. Lett. 80 (2002) 318–319.
[33] D.P. Kim, K.T. Moon, J.G. Kho, J. Economy, C. Gervais, F. Babonneau, Polym. Adv. Technol. 10 (1999) 702–710.
[34] L.J. Bellamy, The Infra-red Spectra of Complex Molecules, Chapman and Hall, London, 1975.
[35] C. Kittel, Introduction to Solid State Physics, 7th ed., John Wiley & Sons, New York, 1996.
[36] L. Pauling, The Nature of the Chemical Bond, Cornell University Press, Ithaca, NY, 1960.
[37] K. Bin-ran Kisohen II, The Chemical Society of Japan, 5th ed., Maruzen, Tokyo, 2004, p. II-741.